Detectors in Nuclear and Particle Physics

Prof. Dr. Johanna Stachel

Department of Physics und Astronomy
University of Heidelberg

June 12, 2018

5. Scintillation counters

5. Scintillation counters

detection of radiation by means of scintillation is among oldest methods of particle detection
historical example: particle impinging on ZnS screen $\rightarrow$ emission of light flash

Principle of scintillation counter:

- $\mathrm{d}E/\mathrm{d}x$ is converted into visible light and transmitted to an optical receiver
  sensitivity of human eye quite good: 15 photons in the correct wavelength range within $\Delta t = 0.1$ s noticeable by human

scintillators make **multipurpose detectors**; can be used in calorimetry, time-of-flight measurement, tracking detectors, trigger or veto counters

Scintillating materials:

- inorganic crystals
- organic crystals
- polymers (plastic scintillators)

5.1 Scintillators

Inorganic crystals: crystal (electric insulator) doped with activator (color center) e.g. NaI(Tl)

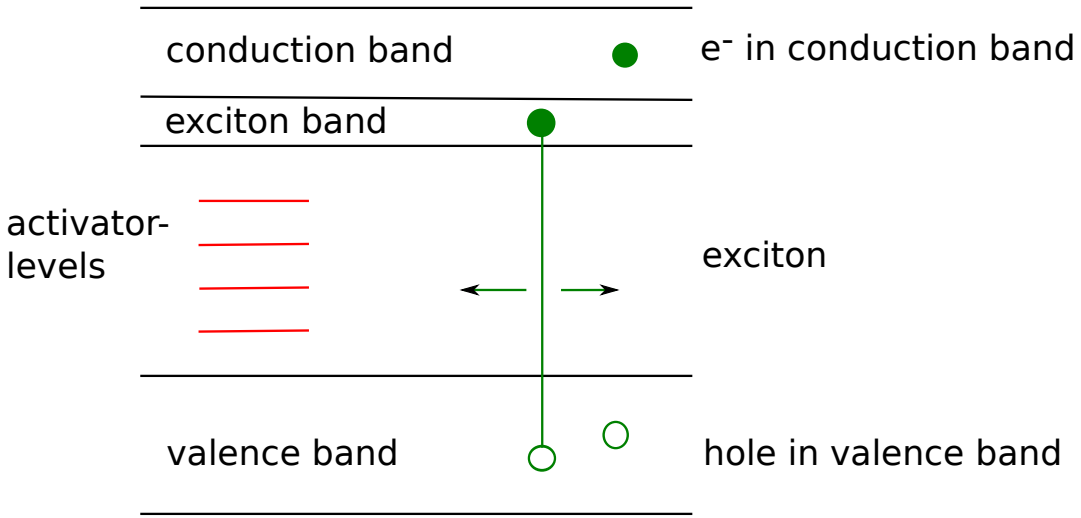

- energy loss can promote electron into conduction band → freely movable in crystal
- also possible: electron remains electrostatically bound to the hole → ≡ 'exciton', hydrogenlike quasiparticle, but much more weakly bound and much bigger, energy levels slightly below conduction band
- exciton moves freely through crystal → transition back into valence band under light emission inefficient process
- doping with activator (energy levels in band gap) to which energy is transferred → photon emission can be much more likely

Inorganic crystals

$$\text{exciton} + \text{activator } A \rightarrow A^* \rightarrow A + \text{photon}$$
$$\text{or } A + \text{lattice vibration}$$

- typical decay time of signal: ns - μs depending on material

  example: NaI(Tl)

$$\begin{aligned} \lambda_{max} &= 410 \text{ nm} \cong 3 \text{ eV} \\ \tau &= 0.23\ \mu\text{s} \\ X_0 &= 2.6 \text{ cm} \end{aligned}$$

- quality of scintillator: light yield $\varepsilon_{sc} \equiv$ fraction of energy loss going into photons

  example: for NaI(Tl) 38000 photons with 3 eV per MeV energy loss (deposit in scint.)

$$\varepsilon_{sc} \cong \frac{3.8 \cdot 10^4 \cdot 3 \text{ eV}}{10^6 \text{ eV}} = 11.3\% \quad \leftarrow \text{good}$$

characteristics of different inorganic crystals

type	λ_{max}[nm]	$\tau[\mu s]$	photons per MeV	X_0[cm]
NaI(Tl)	410	0.23	38000	2.6
CsI(Tl)	565	1.0	52000	1.9
CsI (at 77 K)*	400	0.60	8300	1.85
	310	0.02	74000	1.85
BGO (bismuth germanate)	480	0.35	2800	1.1
BaF_2	310	0.62	6300	2.1
	220	0.0007	2000	2.1
CeF_3	330	0.03	5000	1.7
$PbWO_4$	430	0.01	100	0.9

* at roomtemperature more than factor 100 less light

- advantages of inorganic crystals:
  - high light yield
  - high density → good energy resolution for compact detector
- disadvantage:
  - complicated crystal growth → \$\$\$ (several US\$ per cm^3)

application in large particle physics experiments

- BaBar (SLAC):

  6580 CsI(Tl) crystals
  depth 17 X_0
  total 5.9 m^3
  readout Si photodiode (gain = 1)
  noise 0.15 MeV
  dynamic range 10^4

- CMS (LHC):

  76150 $PbWO_4$ crystals
  26 X_0
  total 11 m^3
  read-out APD (gain = 50)
  noise 30 MeV
  dynamic range 10^5

$PbWO_4$: fast, small radiation length, good radiation hardness compared to other scintillators, but comparatively few photons (order of 10 photoelectrons per MeV)

always need to consider: match of spectral distribution of light emission, absorption and sensitivity of photosensor

typical spectral distributions:

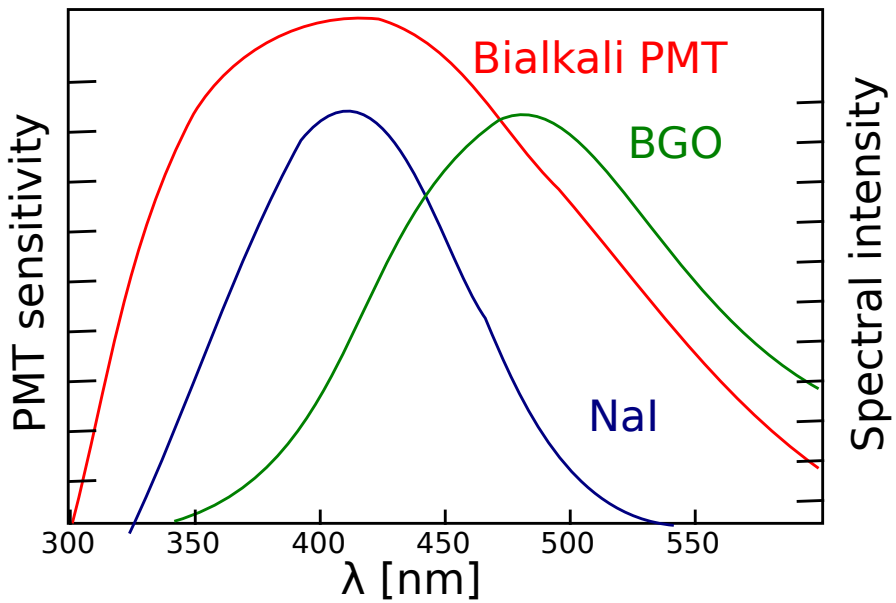

Organic crystals

aromatic hydrocarbon compoints
scintillation is based on the delocalized π electrons of aromatic rings (see below)

	λ_{max}[nm]	τ[ns]	light yield rel. to NaI
naphthalene 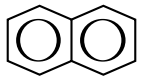	348	96	12%
anthracene 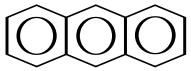	440	30	50%

advantages: relatively fast, cheap, mechanically strong
disadvantages: mechanically difficult to process, light output anisotropic (due to channeling in crystals)

Plastic scintillators

polymer + scintillator + wavelength shifter or liquid + scintillator + wavelength shifter

- **Polymers** (transparent)

  polystyrene

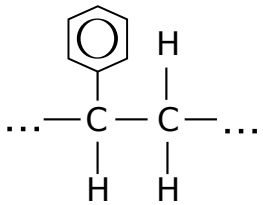

  lucite (plexiglas)

  polyvinyltoluene

- **Liquid** (transparent): benzene, toluene, mineral oil

- **Scintillators**

		λ_{max}[nm]	τ[ns]	ε_{sc}
p-Terphenyl		440	5	25%
PBD 2-phenyl-5(4-biphenyl)-1,3,4-oxadiazole	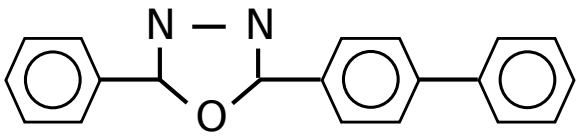	360	1	

disadvantages: low light yield: in plastic scintillator typically 10 photons per 1 MeV energy loss, low radiation length $X_0 = 40 - 50$ cm,
advantages: fast decay time (order of) ns, cheap, easy to shape, typically also high neutron detection efficiency via (n,p) reactions

typical organic scintillators and wavelength shifters:

primary fluorescent agent	structure	λ_{max} emission [nm]	decay time [ns]	light yield rel. to NaI
naphtalene	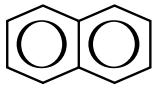	348	96	0.12
anthracene	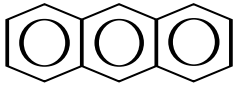	440	30	0.5
p-terphenyl		440	5	0.25
PBD	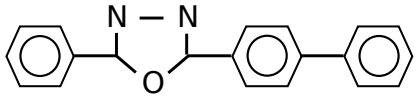	360	1.2	
wavelength shifter				
POPOP	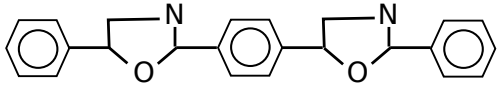	420	1.6	
bis-MSB	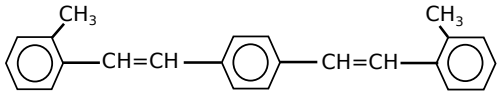	420	1.2	

what does wavelength shifter do?

- it absorbs primary scintillation light and reemits at longer wavelength
  $\rightarrow$ good transparency for emitted light
- adapts wave length to spectral sensitivity of photosensor

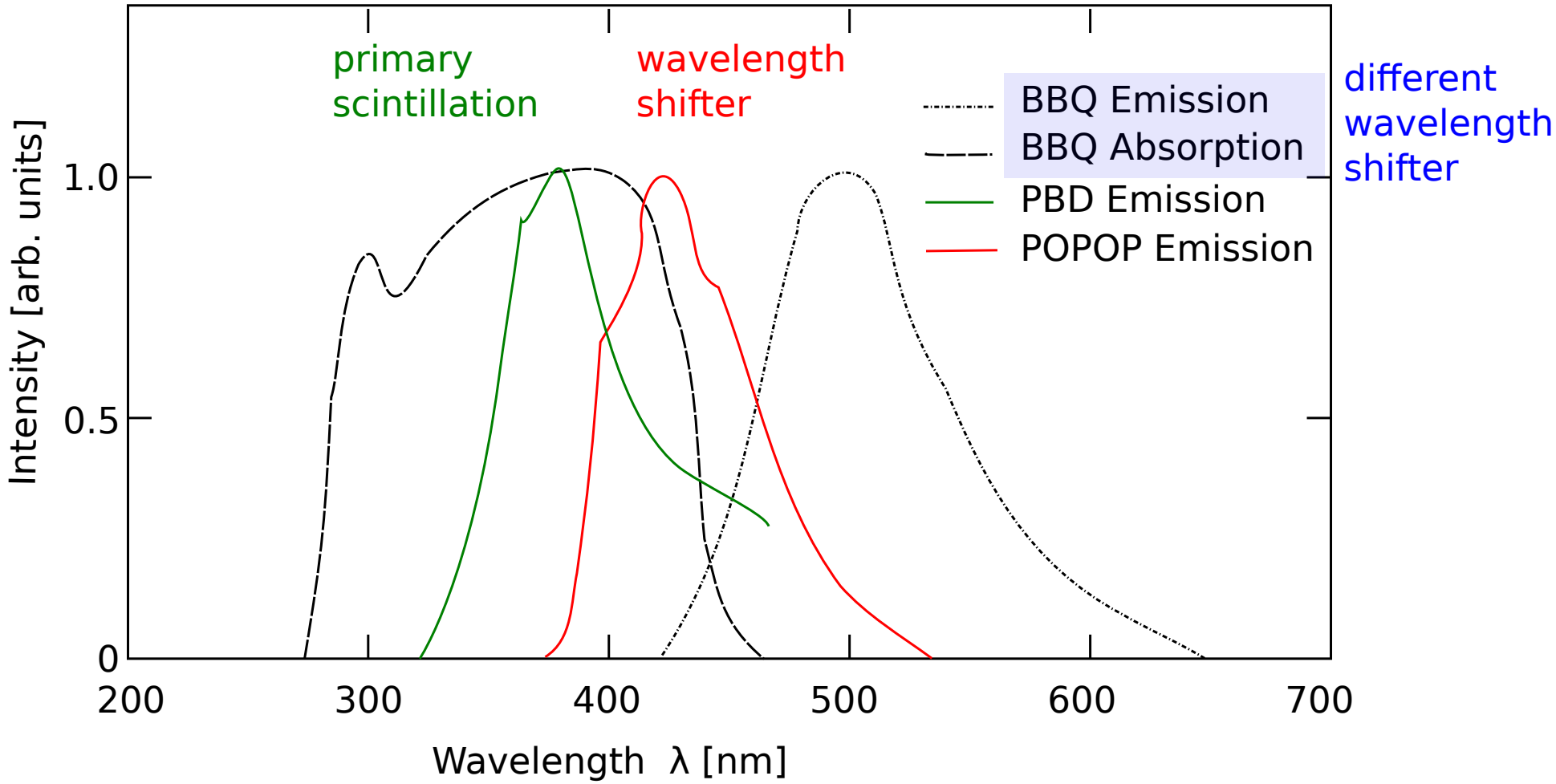

emission spectra of primary fluorescent substance (PBD)
and of two different wavelength shifters, BBQ (benzimidazo-benzisochinolin-7-on) and POPOP (1,4-bis-[2-(5-phenyloxazolyl)]-benzene))
and absorption spectrum of wavelength shifter BBQ

principle of operation of organic scintillator:

aromatic molecules with delocalized π-electrons, valence electrons pairwise in π states, level scheme splits into singlet and triplet states

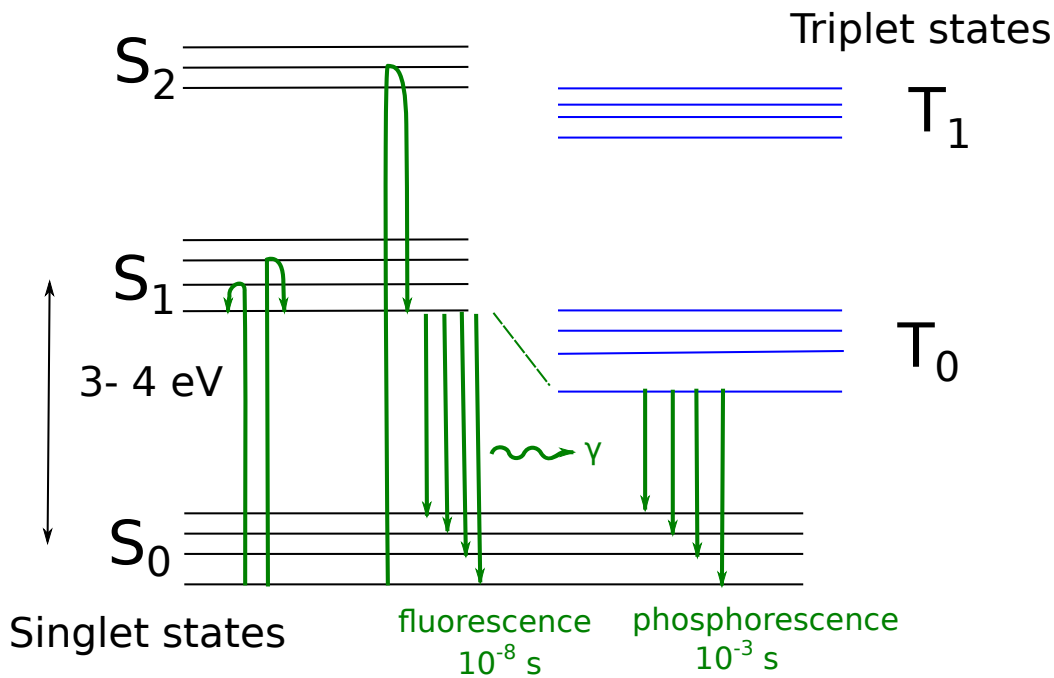

- excitation of π electrons
  energy absorption $\rightarrow S_1^*$, $S_2^* \rightarrow S_1$ radiationless on time scale 10^{-14} s
  fluorescence: $S_1 \rightarrow S_0$
- ionization of π electrons followed by recombination populates T states
  phosphorescence $T_0 \rightarrow S_0$
- excitation of σ-electrons $\rightarrow$ thermal deexcitation, radiationless, collisions and phonons
- other ionization $\rightarrow$ radiation damage

material transparent for radiation with $E_\gamma < S_1^0 - S_0^0$

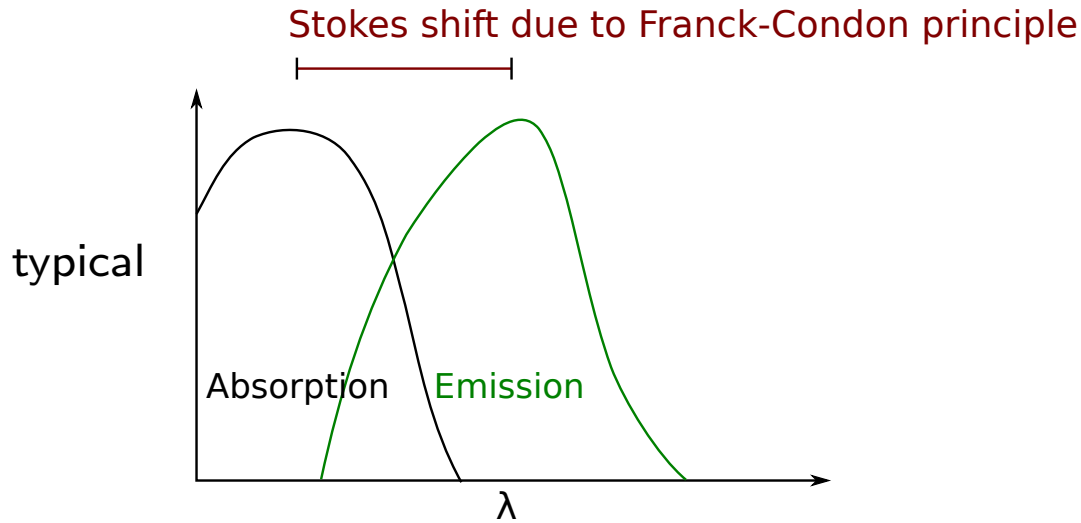

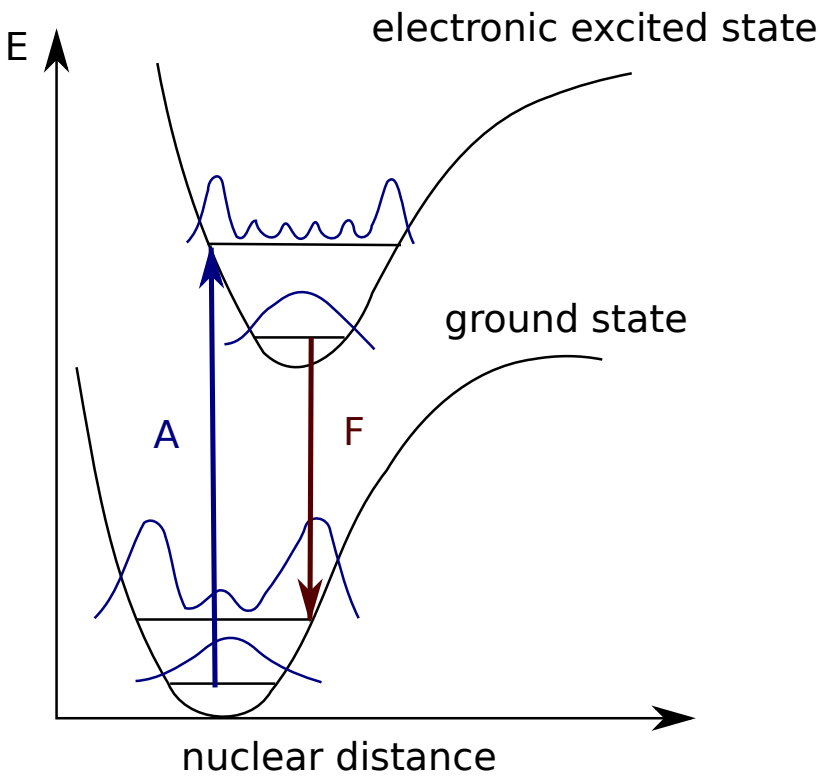

excitation on time scale 10^{-14} s
typical vibration time scale 10^{-12} s
typical S_1 lifetime 10^{-8} s
excitation into higher vibrational state
deexcitation from lowest vibrational state

in base material energy deposit
→ excitation
generally bad light yield

transfer of excitation to primary fluorescent

primary fluorescent
good light yield

absorption spectrum needs to be matched to excited states in base material

depending on material, a secondary fluorescent (wavelength shifter) is introduced to separate emission and absorption spectrum (transparency)

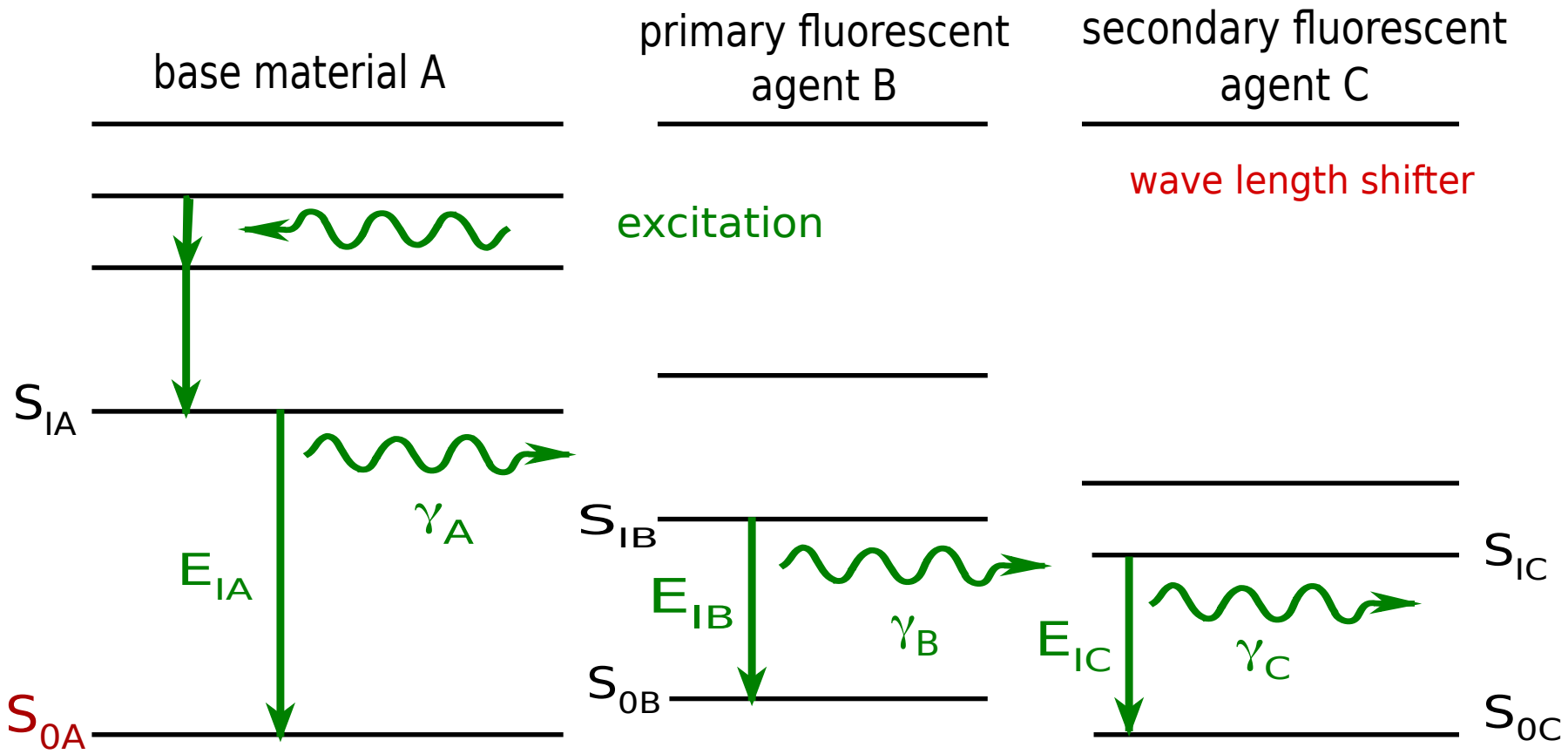

Scintillating gases

- many gases exhibit some degree of scintillation

	λ_{max} [nm]	γ/4.7 MeV α
N_2	390	800
He	390	1100
Ar	250	1100

contributes in gas detector to electric discharge, and be careful in Cherenkov detectors!

Pierre Auger Observatory for cosmic-ray-induced air-showers: employs water Cherenkov detectors and fluorescence detectors to observe UV fluorescence light emitted by atmospheric nitrogen (up to 4 W at maximum of cascade)

- liquid noble gases: lAr, lKr, lXe also scintillate
  in UV (120-170 nm), good light yield (40 000 photons per MeV),
  fast (0.003 and 0.022 μs)

usage in (sampling) calorimeters

5.2 Photon detection

5.2.1 Photomultiplier

i) photo effect in photocathode: $\gamma + \text{atom} \rightarrow \text{atom}^+ + e^-$

$$T_e = h\nu - W$$

W: work function, in metals $3 - 4$ eV, bad! comparable to energy of scintillation photon

$\Rightarrow$ specially developed alloys (bialkali, multialkali) with $W = 1.5 - 2$ eV

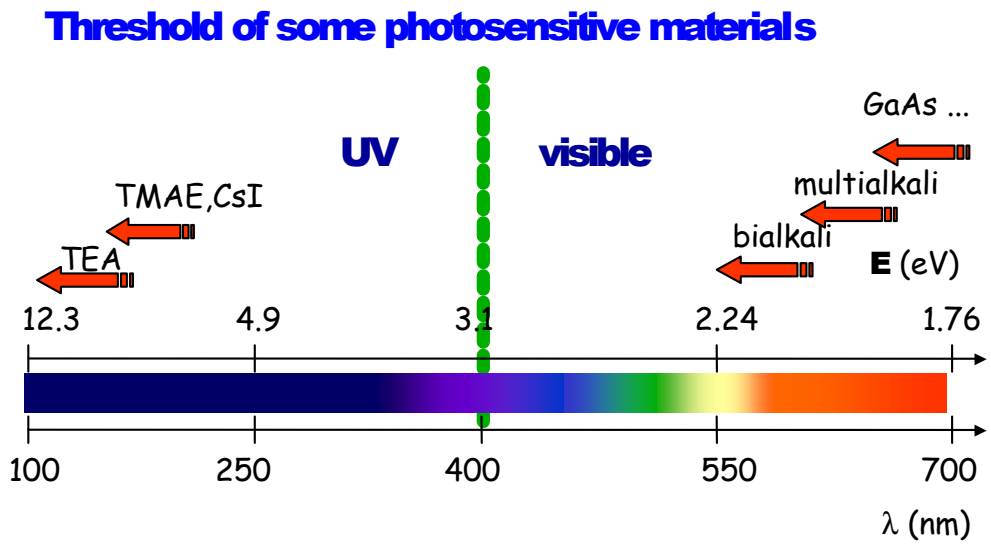

figure of merit: quantum yield

$$Q = \frac{\#\text{photoelectrons}}{\#\text{photons}} \cong 10 - 30\%$$

typical spectral sensitivity

cut-off at small wavelength: glass window can be replaced by quartz, extending range to smaller wavelengths (see e.g. fast component of light of BaF_2)

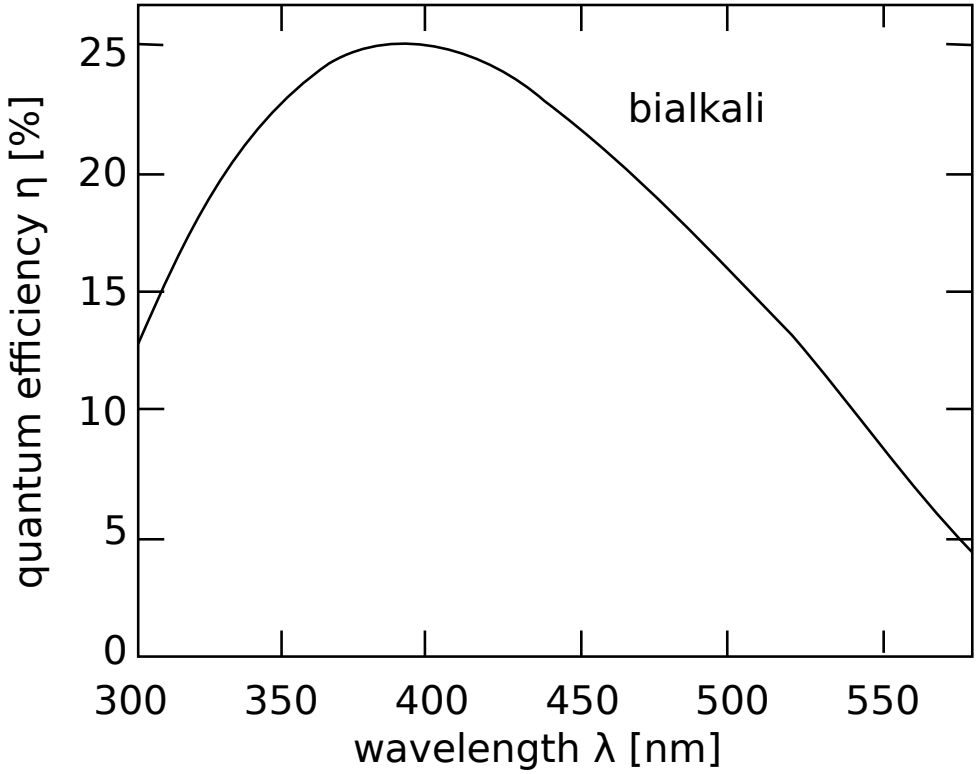

spectral sensitivity (quantum efficiency) of a bialkali (SbKCs) photocathode as a function of the wavelength

also used:

- SbRbCs
- SbCs
- $SbNa_2KCs$ (multialkali)

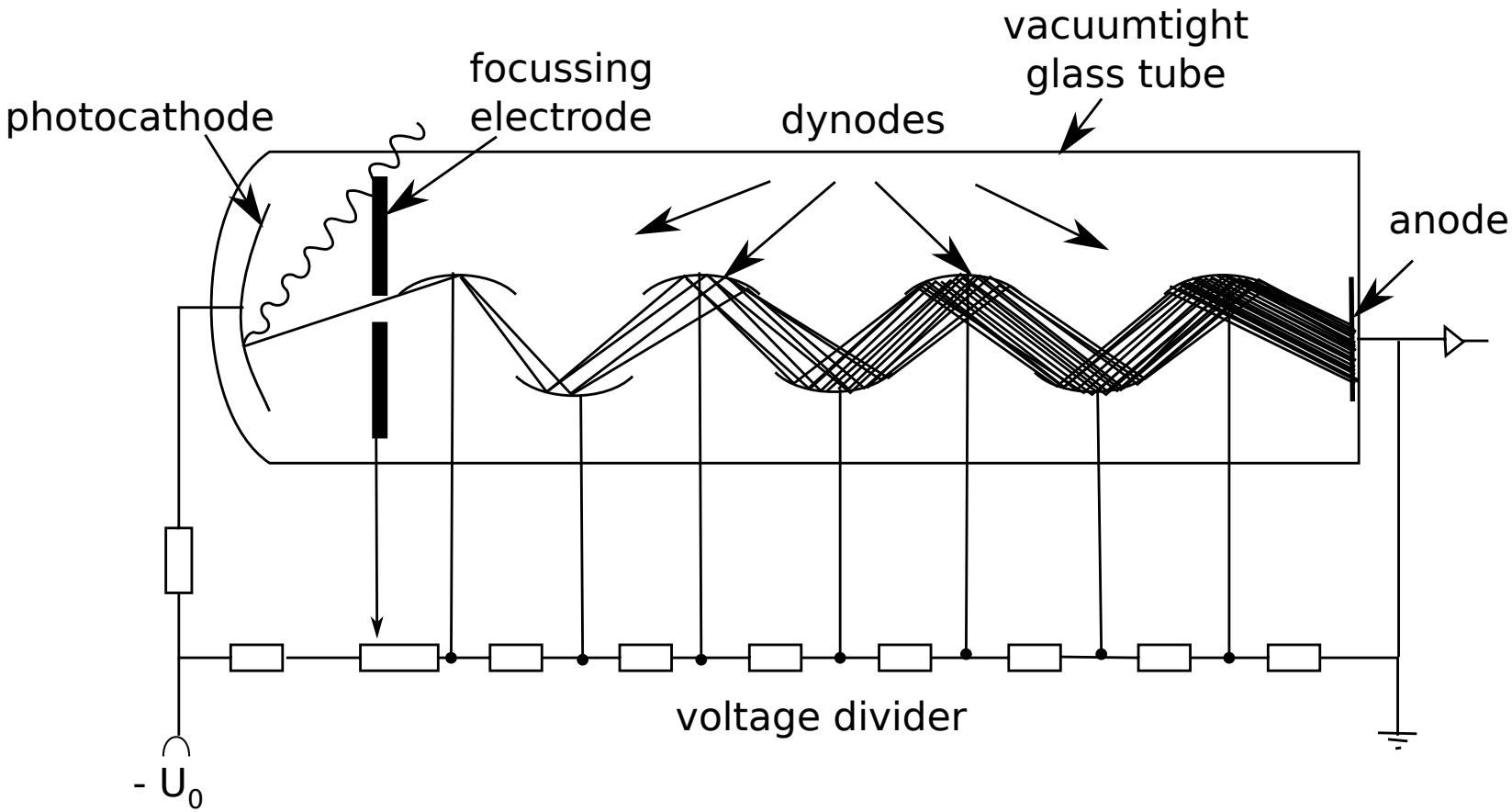

<u>working principle of a photomultiplier</u> electrode system mounted in an evacuated glass tube

photomultiplier usually surrounded by a μ-metal cylinder (high permeability material) to shield against stray magnetic fields (e.g. the magnetic field of the earth)

ii) multiplication of photoelectrons by dynodes

- electrons are accelerated towards dynode
- knock out further electrons in dynode

secondary emission coefficient $\delta = \dfrac{\#\text{ leaving } e^-}{\#\text{ incident } e^-}$

$$\left.\begin{array}{ll}\text{typically} & \delta = 2-10 \\ \#\ \text{dynodes} & n = 8-15\end{array}\right\} \quad G \propto \delta^n = 10^6 - 10^8$$

δ dependent on dynode potential difference:

$$\delta = k \cdot U_D$$

$$G = a_0 (k U_D)^n \qquad a_0 : \text{ collection efficiency between cathode and first dynode}$$

operational voltage $U_B = nU_D$ dynodes connected via resistive divider chain

$$\frac{dG}{G} = n\frac{dU_D}{U_D} = n\frac{dU_B}{U_B}$$

Limitations in energy measurement

- linearity of PMT: at high dynode current possibly saturation by space charge effects $I_A \propto n_\gamma$ for 3 orders of magnitude possible
- photoelectron statistics for mean number of photoelectrons n_e given by Poisson distribution

$$P_n(n_e) = \frac{n_e^n \exp(-n_e)}{n!}$$

with good PMT, observation of single photoelectrons possible

photoelectron statistics for a given energy loss dE/dx respectively E_γ defined by

$$n_e = \frac{dE}{dx} \times \frac{\text{photons}}{\text{MeV}} \times \text{ light collection efficiency } \times \text{ quantum efficiency}$$

e.g. in NaI(Tl) for 10 MeV incident photon:

$$n_e = 10\ \text{MeV} \times \frac{38000}{\text{MeV}} \times 0.2 \times 0.25 = 15000$$

$$\frac{\sqrt{n_e}}{n_e} = 0.8\%$$

- fluctuations of secondary electron emission at mean multiplication factor δ (again Poisson)

$$P_n(\delta) = \frac{\delta^n \exp(-\delta)}{(n!)} \qquad \text{for Poisson with mean } \langle n \rangle = \delta$$

$$\text{variance} \quad \sigma_n^2 = \langle n \rangle = \delta$$

contribution to resolution $\quad \frac{\sigma_n}{\langle n \rangle} = \frac{1}{\sqrt{\delta}}$

N stages of dynodes which each amplify by factor δ:

$$\left(\frac{\sigma_n}{\langle n \rangle}\right)^2 = \frac{1}{\delta} + \frac{1}{\delta^2} + \ldots + \frac{1}{\delta^n} = \frac{1-\delta^{-N}}{\delta - 1} \cong \frac{1}{\delta - 1}$$

$$\frac{\sigma_n}{\langle n \rangle} = \frac{1}{\sqrt{\delta - 1}}$$

quality of PM dominated by first stage

Pulse shape:

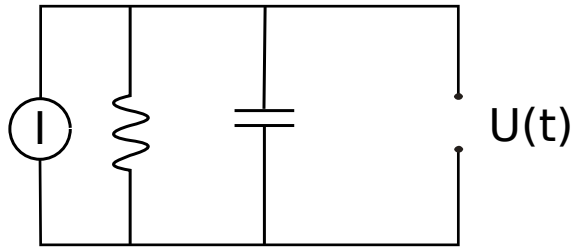

ideal current source with parallel resistance R and capacitance C

light incident with decay time of scintillator τ_{sc}

$$N_\gamma = N_0 \exp\left(-t/\tau_{sc}\right)$$

anode current
$$I(t) = \frac{G n_e e}{\tau_{sc}} \exp\left(-t/\tau_{sc}\right) = I_0 \exp\left(-t/\tau_{sc}\right)$$

$$Q = \int I \mathrm{d}t = I_0 \tau_{sc} = G n_e e$$

$$I(t) = \frac{U(t)}{R} + C \frac{\mathrm{d}U(t)}{\mathrm{d}t}$$

$\rightarrow$ voltage signal (with $U(t=0) = 0$)

$$\boxed{U(t) = \frac{Q \cdot R}{\tau - \tau_{sc}} \left[\exp\left(-\frac{t}{\tau}\right) - \exp\left(-\frac{t}{\tau_{sc}}\right)\right]} \qquad \tau = RC$$

2 possible realizations (limiting cases) optimized for i) pulse height or ii) timing:

i) $RC = \tau \gg \tau_{sc}$

$$U(t) = \frac{Q}{C}\left(\exp\left(-\frac{t}{\tau}\right) - \exp\left(-\frac{t}{\tau_{sc}}\right)\right)$$
$$= \begin{cases} \frac{Q}{C}\left(1 - \exp\left(-\frac{t}{\tau_{sc}}\right)\right) & \tau \gg t \\ \frac{Q}{C}\exp\left(-\frac{t}{\tau}\right) & t \gg \tau_{sc} \end{cases}$$

rising edge of pulse characterized by τ_{sc} linear in t
pulse length characterized by $\tau = RC$

$$U_{max} \cong Q/C \propto N_\gamma \quad \rightarrow \quad \boxed{\textbf{energy measurement}}$$

ii) $RC = \tau \ll \tau_{sc}$

$$U(t) = \frac{\tau}{\tau_{sc}}\frac{Q}{C}\left(\exp\left(-\frac{t}{\tau_{sc}}\right) - \exp\left(-\frac{t}{\tau}\right)\right)$$
$$= \begin{cases} \frac{\tau}{\tau_{sc}}\frac{Q}{C}\left(1 - \exp\left(-\frac{t}{\tau}\right)\right) & t \ll \tau_{sc} \\ \frac{\tau}{\tau_{sc}}\frac{Q}{C}\exp\left(-\frac{t}{\tau_{sc}}\right) & t \gg \tau \end{cases}$$

rising edge of pulse given by small RC, again linear in t
decay of pulse given by τ_{sc} $\rightarrow$ $\boxed{\textbf{time measurement}}$
sensitivity to Q/C weakened by small RC

time resolution given by:

- rise time of signal (order $1 - 2$ ns)
- transit time in photomultiplier (order $30 - 50$ ns)
  respectively, variations in transit time (order 0.1 ns for good PMT)

transit time variations via

- path length differences cathode - first dynode

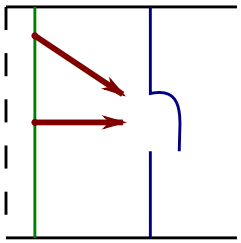

$\Delta t \cong 1$ ns for cathode $\varnothing$ 10 cm
5 ns $\varnothing$ 50 cm

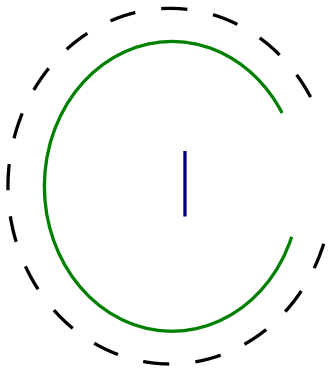

hence spherical arrangement for very large PMTs
(e.g. 20" in Superkamiokande)

- energy spread of photoelectrons when they leave the photocathode
  timing difference for photoelectron accelerated from rest
  ($T_e = 0$) relative to one with T_e

$$\Delta t = \frac{\sqrt{2mT_e}}{eE}$$

therefore maximize potential difference between cathode and first dynode, e.g.

$$T_e = 1 \text{ eV} \qquad E = 200 \text{ V/cm} \quad \rightarrow \quad \Delta t = 0.17 \text{ ns}$$

strong reduction of pathlength difference:
"micro channel plate"

arrangement of $10^4 - 10^7$ parallel channels (glass tubes)
of $10 - 50$ μm diameter, $5 - 10$ mm length

electric field inside by applying voltage to one end ($\sim$ 1000 V) and coated inside with resistive layer acting as a continuous dynode

realization: holes in lead glass plate

$$G = 10^5 - 10^6 \qquad \Delta t = 0.1 \text{ ns}$$

further advantage: can be operated inside magnetic field

difficulty: positive ions created by collisions with rest gas inside channel must be prevented from reaching photo cathode (otherwise death of MCP) $\rightarrow$ extremely thin ($5 - 10$ nm) Al window between channel plate and photocathode

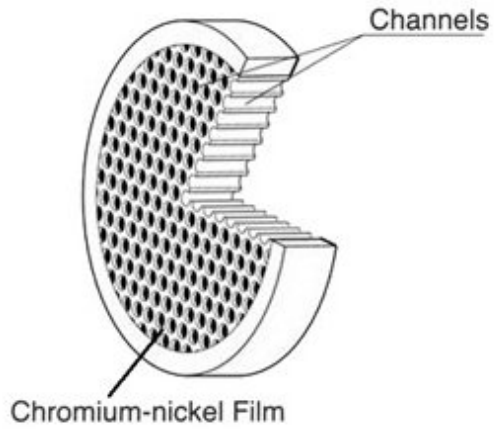

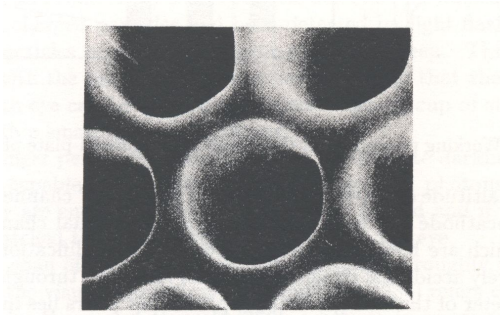

Fig. 5.6. Microphotograph of microchannels [384].

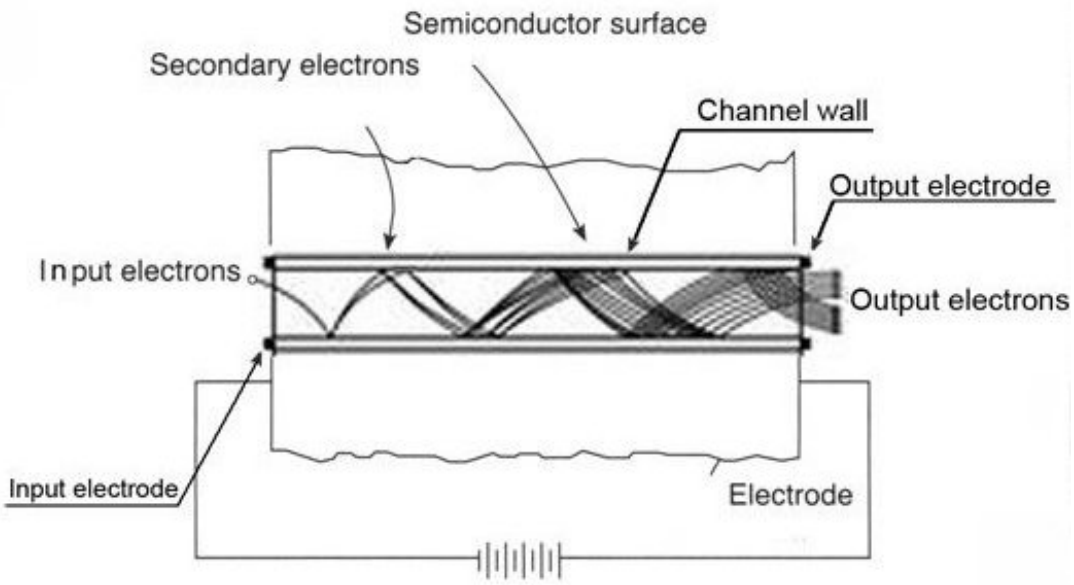

characteristics for several commercially available PMTs and microchannel plates

	Amperex XP 2020	RCA 8854	Hamamatsu R 647-01	ITT F 4129	Hamamatsu R 1564U
amplification	$> 3 \cdot 10^7$	$3.5 \cdot 10^8$	$> 10^6$	$1.6 \cdot 10^6$	$5 \cdot 10^5$
HV anode-cathode (V)	2200	2500	1000		
microchannel voltage (V)				2500	3400
rise time τ_R (ns)	1.5	3.2	2	0.35	0.27
transit time τ_T (ns)	28	70	31.5	2.5	0.58
transit time variation τ_S, one PE	0.51	1.55	1.2	0.20	0.09
transit time variation τ'_S, many PEs	0.12		0.40	0.10	
number of PEs for transit time τ'_S meas.	2500		100	800	
quantum yield (%)	26	27	28	20	15
photocathode diameter (mm)	44	114	9	18	18
dynode material	Cu Be	GaP/BeO			

time resolution influenced by transit time variation and dimensions of scintillator (timing variation of light collection):

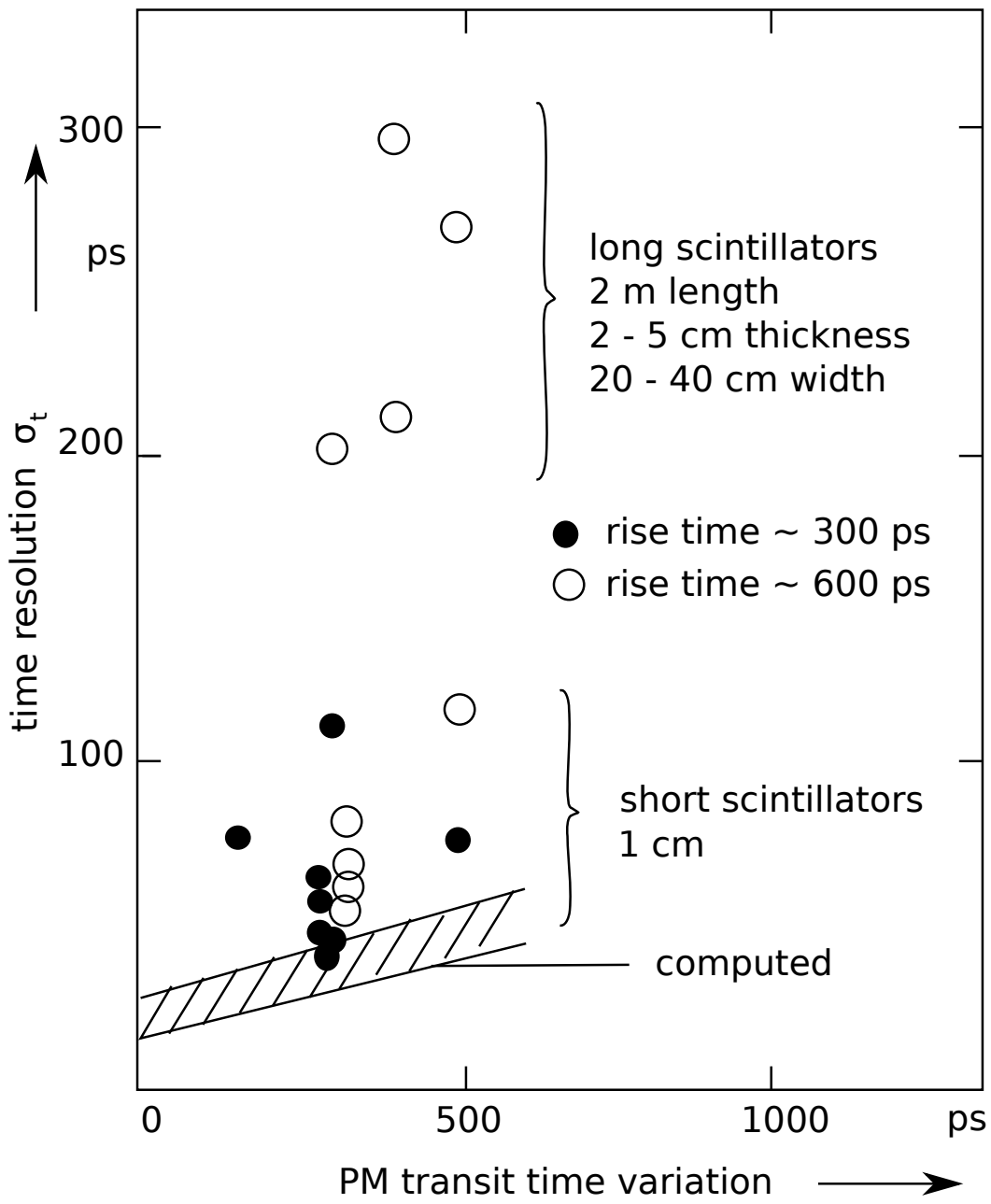

different light paths in scintillator:

affect both time resolution and pulse height
typical attenuation length about 1 m
attenuation mostly at short wavelengths

⇒ use of yellow filter reduces dependency

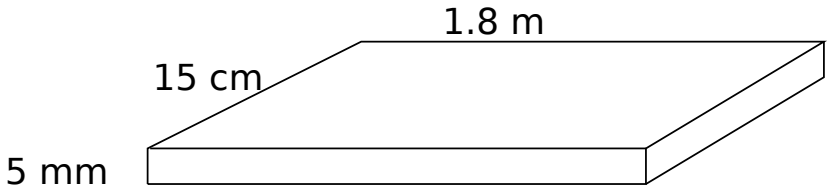

also: read-out of long scintillator at both ends reduces both timing variations and spatial dependence of pulse height

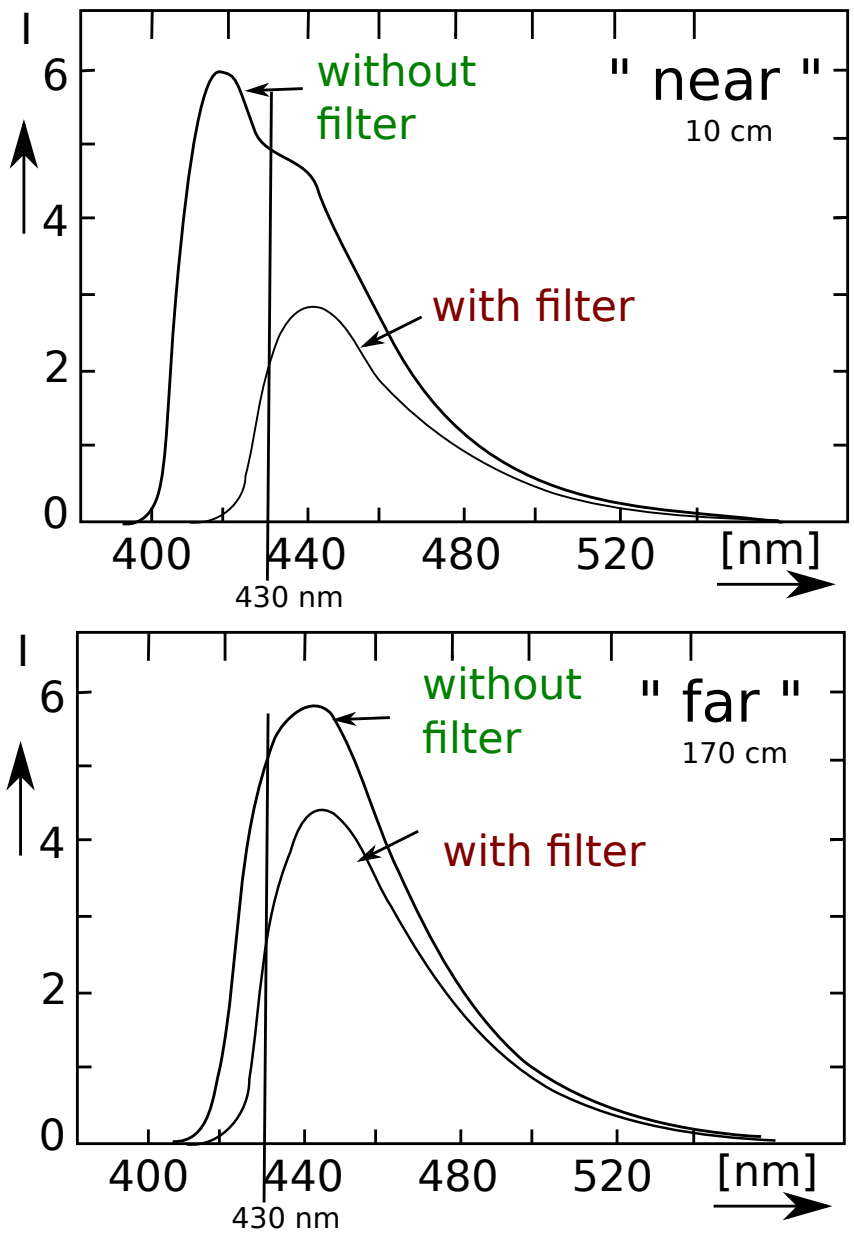

amplitude distribution with and without yellow filter in front of cathode

Photomultipliers in magnetic field

B-field disturbs focusing of photoelectrons and secondary electrons
typical kinetic energies $T \leq 200$ eV
in region of dynodes: $B \leq 10^{-4}$ T needed
typical magnitude of effect: $B = 0 \rightarrow 0.15 \cdot 10^{-4}$ T means $I_A \rightarrow \frac{1}{2} I_A$

solution: small fields can be shielded by so-called μ-metal

use of mesh-type dynodes ($\vec{E}$ and $\vec{B}$ parallel)

use of channel plate, photodiodes, silicon-PM, or hybrid photon-detectors (see journal club for the latter two)

5.2.2 Photodiodes

normal photodiode: PIN type gain $= 1$,
i.e. each photoelectron contributes 1 e to final signal (see chapter 4)

avalanche photodiode (APD): typical gain $= 30 - 50$ (CMS EMCal)
amplification of photocurrent through avalanche multiplication of carriers in the junction region (high reverse bias voltage, 100-200 V)

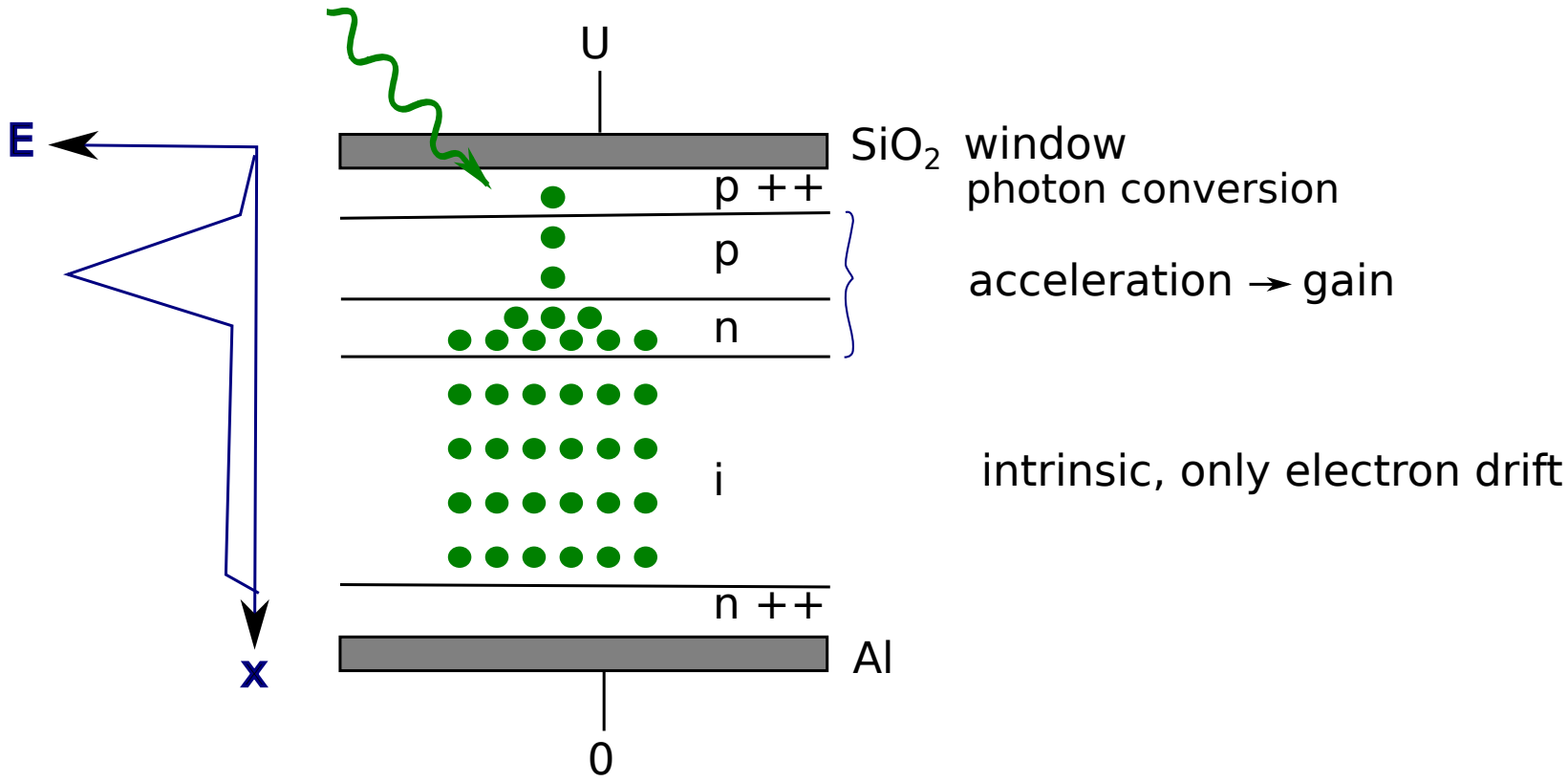

5.3 Propagation of light

- in scintillator itself:
  - absorption $N_\gamma = N_0 \exp(-x/L)$
    with L: absorption length
  - reflection at the edge, total reflection for
    $$\theta > \theta_{tot} = \arcsin(n_0/n_s)$$

  in typical scintillator $n \cong 1.4$, $\theta_{tot} \cong 45°$

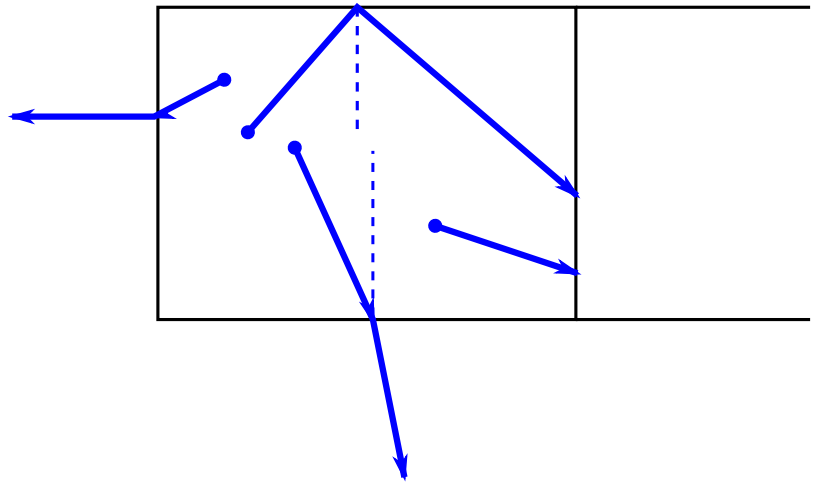

- light guide
  - the light exiting the scintillator on one end (rectangular cross section) needs to be guided to PMT (normally round cross section) $\Rightarrow$ 'fish tail' shape

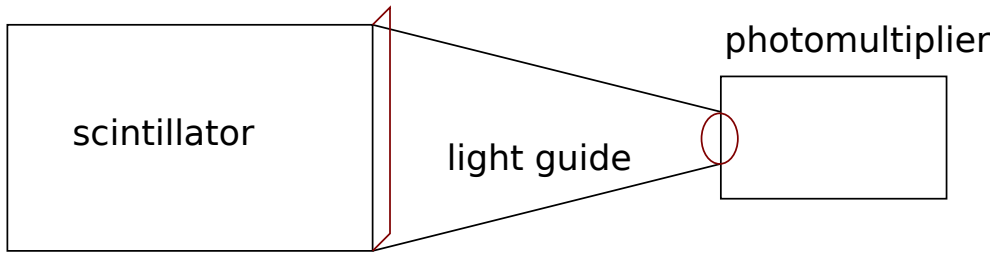

Light guide

Liouville theorem is valid also for guiding light:

$$\Delta x \cdot \Delta\theta_x = \text{const.}$$

i.e. product of width and divergence is constant

for guiding light $\Delta\theta = \text{const}$,
Δx must not decrease, otherwise loss of light,
so keep area constant

curvature should only be weak to maintain
total reflection for photons captured once
(adiabatic light guide)

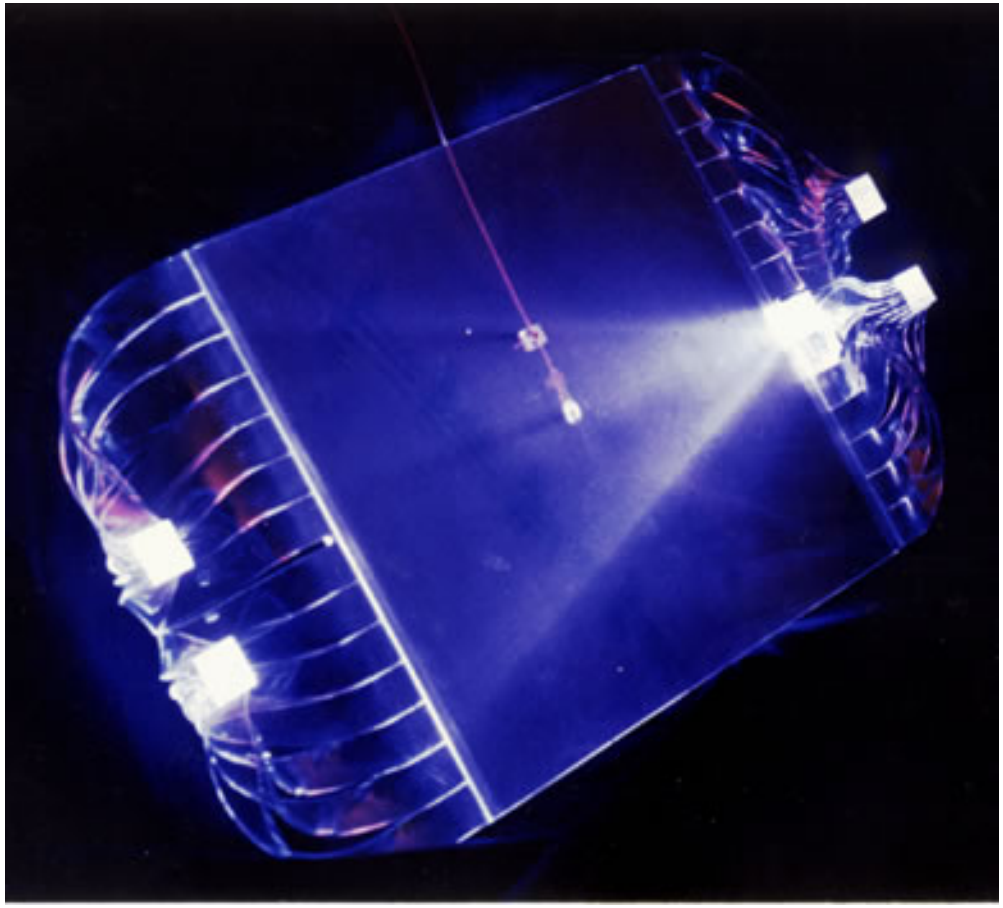

Wavelength shifter

when enough light: can use 2nd wavelength shifter, e.g. along edge of scintillator plate, wavelength shifter rod absorbs light leaving scintillator and reemits isotropically at (typically) green wavelength, small part $(5 - 10\%)$ is guided to PMT
advantage: can achieve very long attenuation length this way, correction small

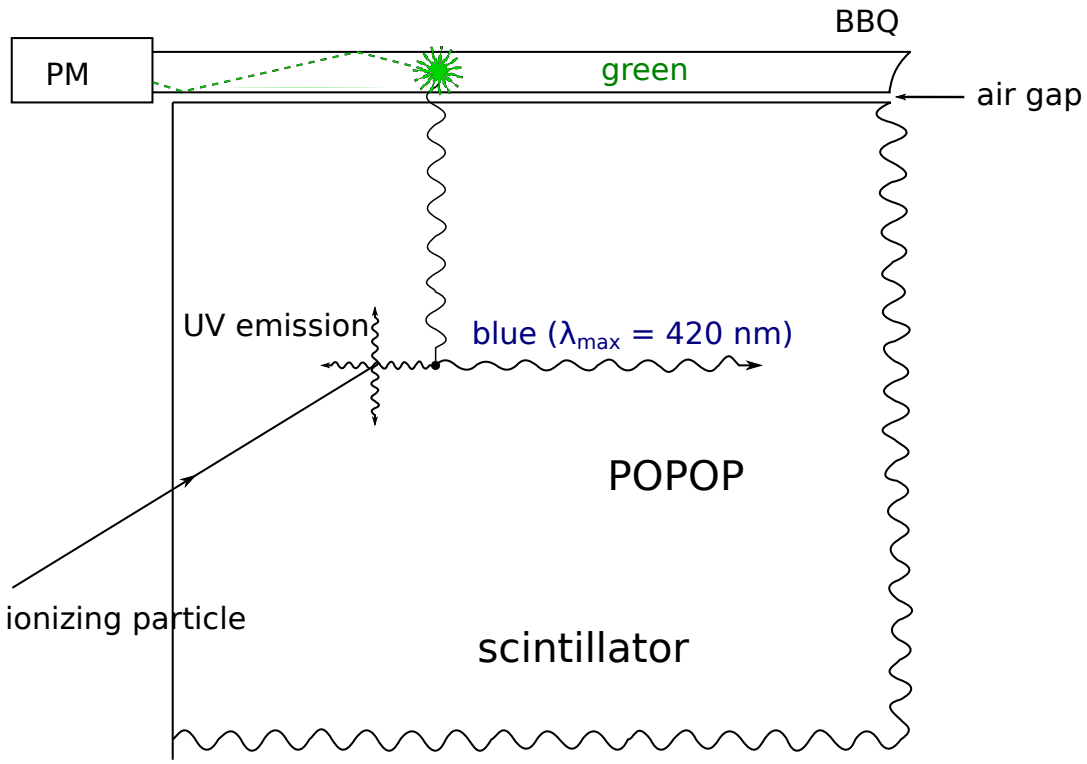

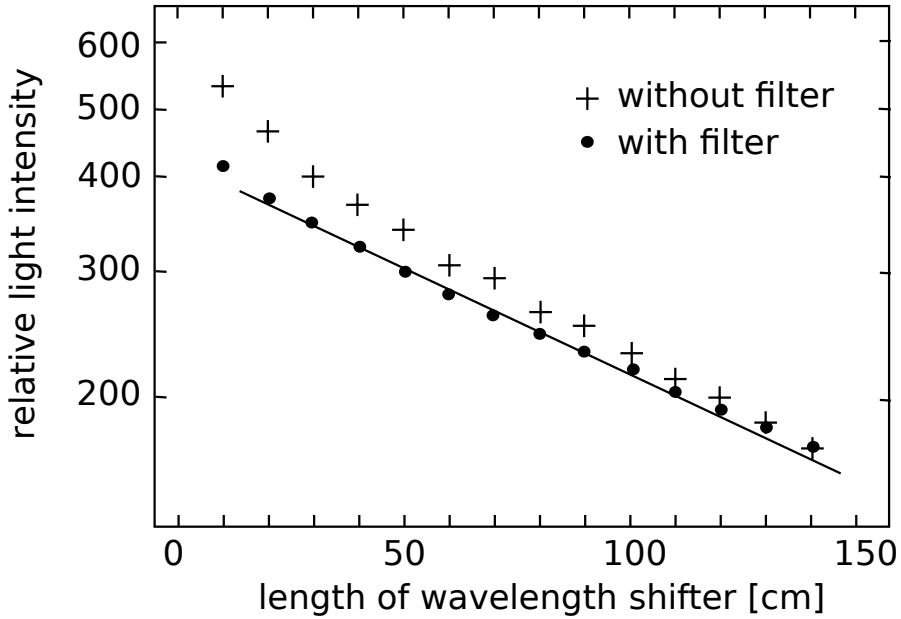

light absorption in 3 mm thick BBQ wavelength shifter rod:
better uniformity of light collection by giving up shorter wavelength component (yellow filter)

5.4 Applications of scintillation detectors

- time-of-flight measurement, 2 scintillation counters (read-out on both ends) at large enough distance
- precise photon energy: crystal calorimeter
- sampling calorimeter for photons and hadrons: alternating layers of absorber (Fe, U, ...) and scintillator with wavelength shifter rods and PMTs
- scintillating fibre hodoscope: layers of fibres, diameter order 1 mm or less, precision tracking, fast vertexing

Sampling calorimeter (see Chapters 8/9)

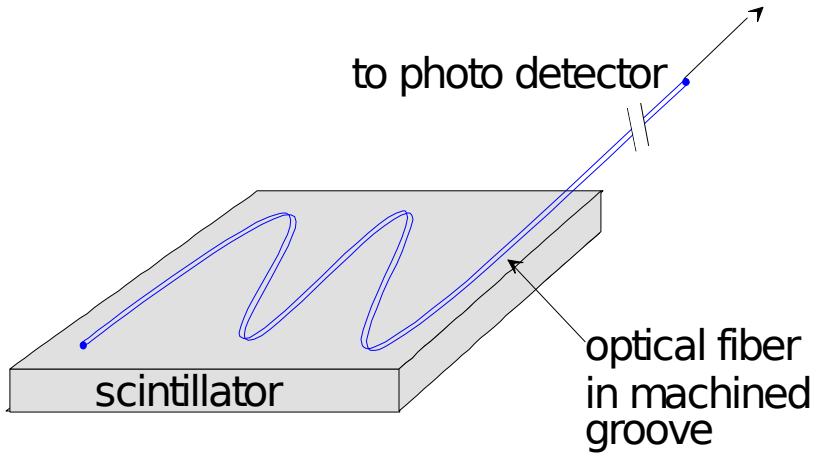

- typically enough light available and uniformity of response and linearity more important
- light emerging from end of scintillator sheet absorbed by external wavelength shifter rod and reemitted isotropically
- air gap essential for total internal reflection
- only a few % of energy loss in light

wavelength shifter rods can be replaced by wavelength shifting scintillating fibers embedded into scintillator sheet or directly into absorber

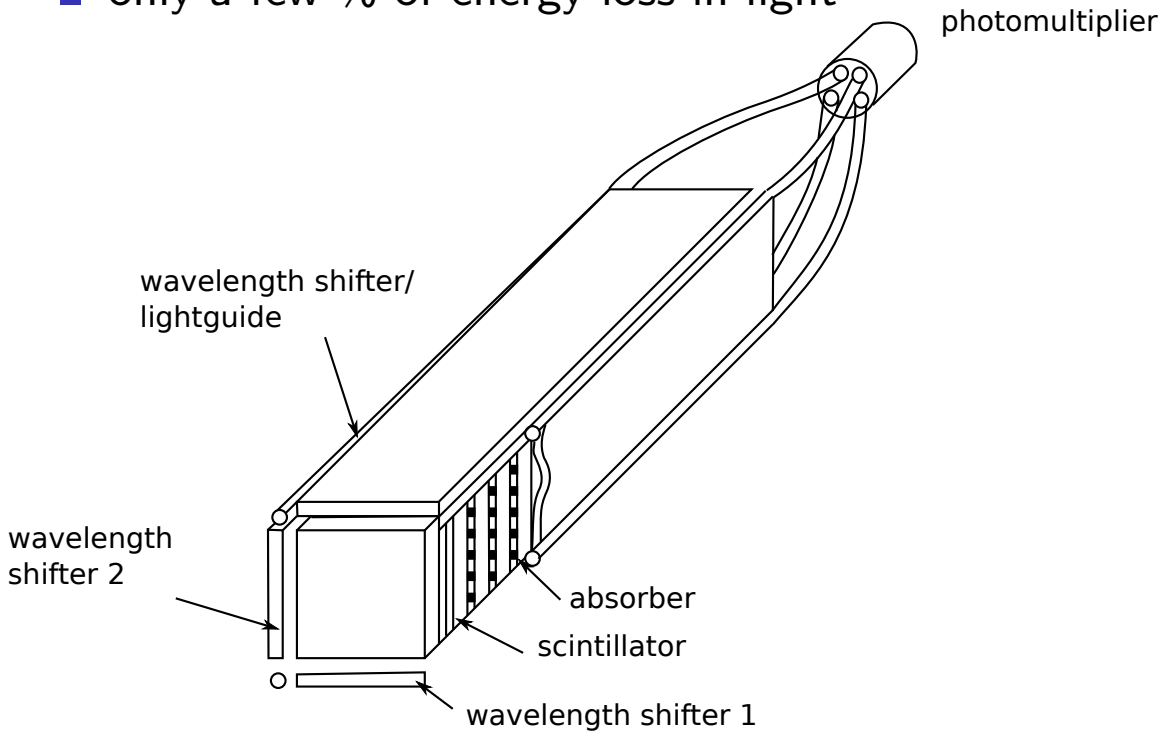

Scintillating fibre hodoscopes

follow track of a charged particle in fine steps but not in gas detector

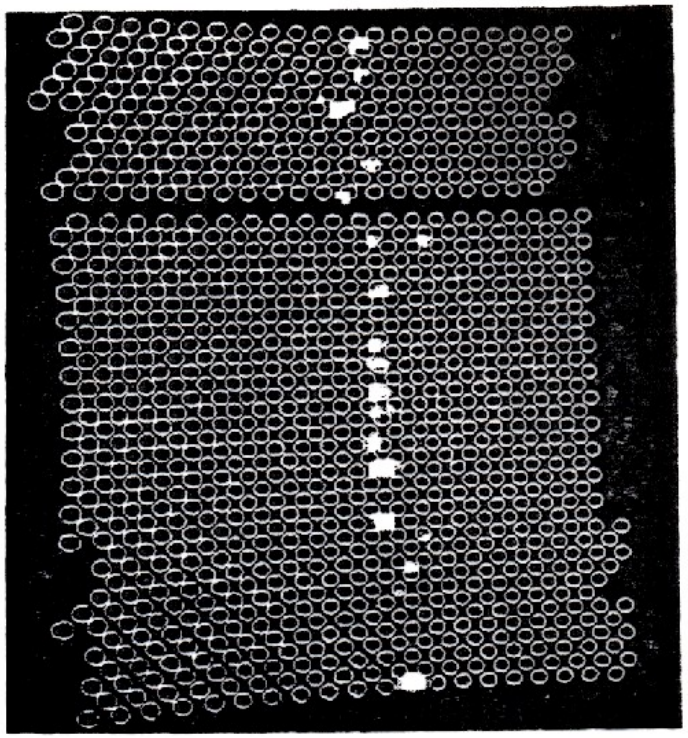

track in scintillating fibre array, fibre diameter 1 mm

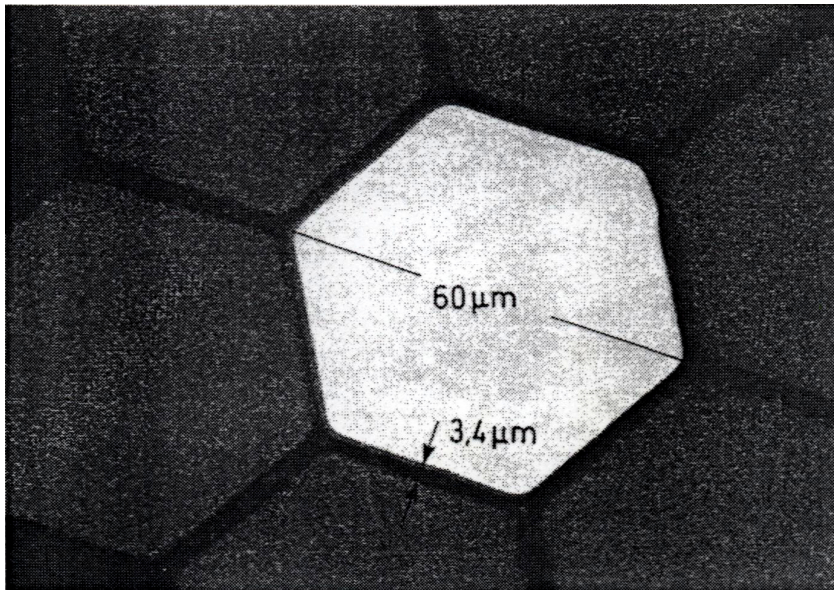

60 μm fibre in a fibre bundle covered with cladding of lower n, single track resolution few tens of μm

Example: Scintillation fibre hodoscope COMPASS at CERN SPS

cover beam area of a $100 - 200$ GeV muon beam, 10^8 Hz or 10^6 Hz per fiber channel

J. Bisplinghoff et al., NIM A490 (2002) 101

to provide enough photoelectrons 4 layers of fibres of 1 mm diameter
fibres in each column joined to same PMT pixel of a multianode PMT
$\rightarrow$ 30 photoelectrons per muon

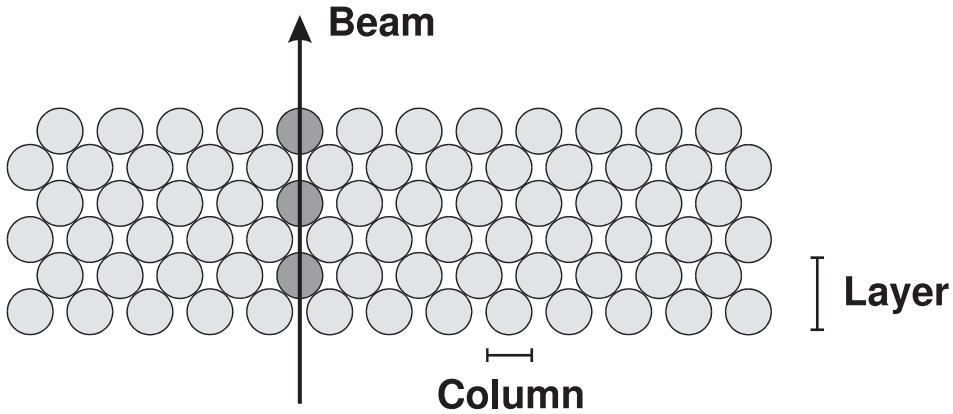

fibre configuration for scintillating fibre hodoscope with 3 layers of fibers

SCSF-78MJ scintillating fibers, 1.5 m attenuation length, active area about 10×10 cm^2, then light guides of clear fibers 1.5 m long (attenuation length 4 m) to PMT

high radiation tolerance (important for beam hodoscope): 100 kGy (10 Mrad) lead to only 15% reduction of signal.

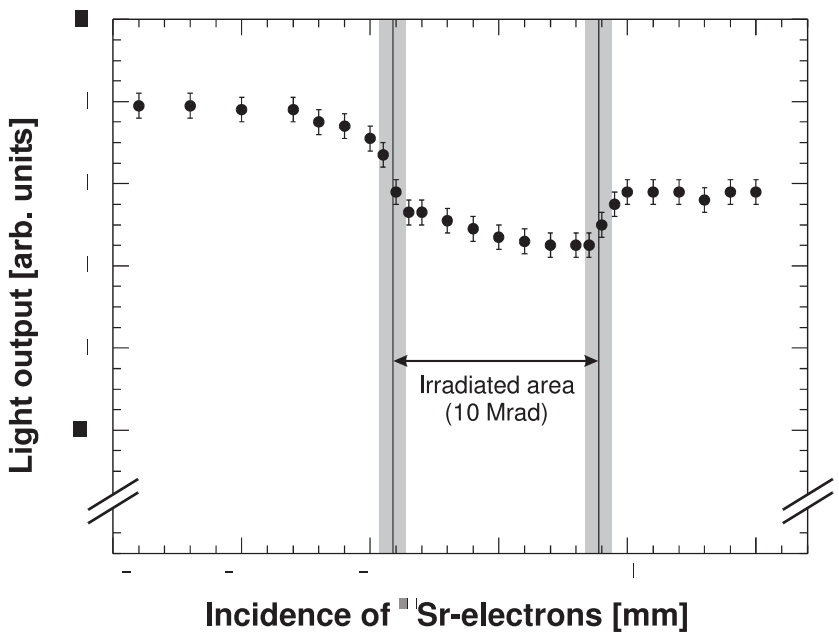

light output of Kuraray SCSF-78MJ scintillating fibers after local irradiation ($\approx$ 100 kGy), as indicated by shaded vertical bars

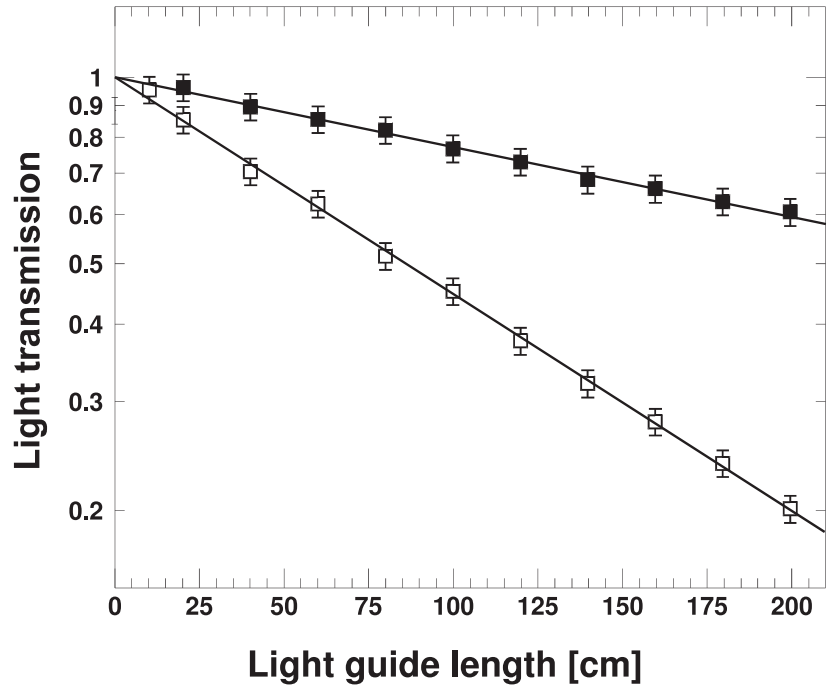

light attenuation of light guides (clear fibers PSMJ, Kuraray Corp.), as measured before (solid squares) and after (open squares) about 10 kGy of irradiation (more than 10 times what is expected for beam halo), homogeneously applied across the entirely of their length.

attentuation length of lightguide drops from 4 m to 1.2 m

'price' for light-saving use of clear fibers:
an additional joint → glue

glue not radiation hard (yellows)
→ needed to learn to 'fuse' fibers

Hamamatsu 16-anode PMT was a breakthrough in gain uniformity and cross talk

H6568 MA-PMT: equipped with a common photocathode followed by 16 metal channel dynodes each with 12 stages of mesh type and a multi-anode read-out. They are arranged as a 4×4 block (individual effective photocathode pads with an area of 4 mm $\times$ 4 mm each and a pitch distance of 4.5 mm (see figure).

figure: layout and dimensions of the multi-channel photomultiplier tube H6568. The upper part shows the front view of the cathode grid.

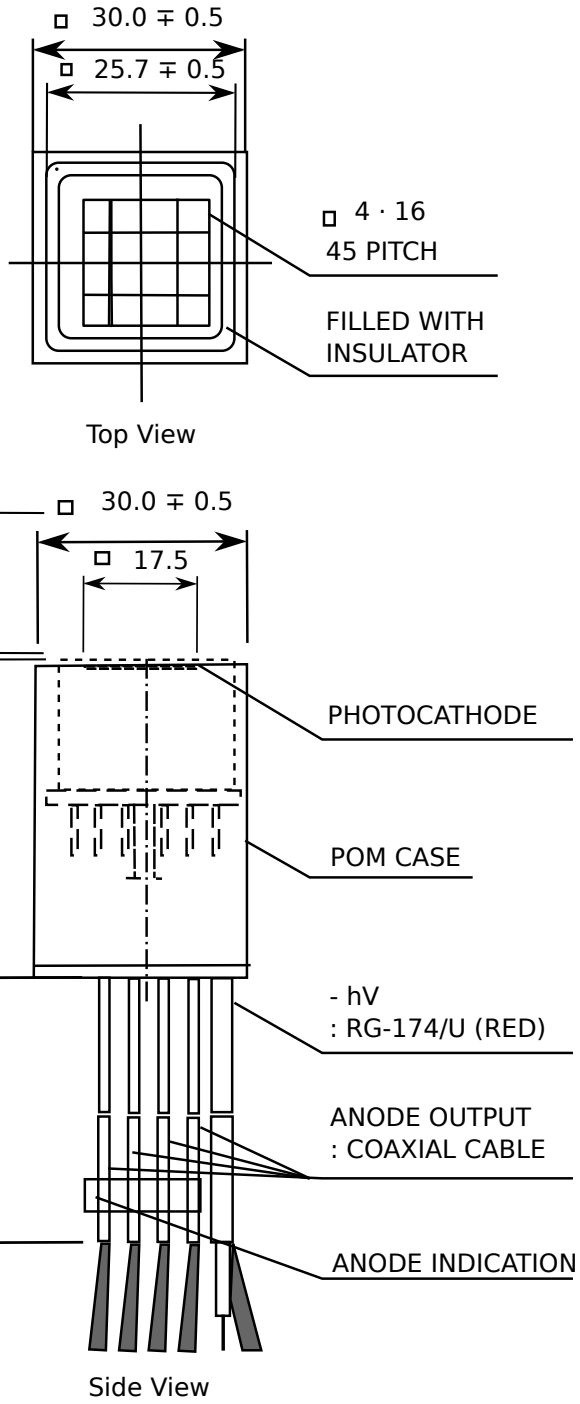

noise only 1/5 of single photoelectron response (SER)

low cross talk (less than 5 %)

good gain uniformity (about 20 %)

voltage divider for dynodes needs to be specifically designed to be stable at rates up to 100 MHz

'active base' (use of transistors instead of resistors for last stages) instead of simple voltage divider, otherwise drop of signal with rate due to large currents through last dynodes leading to drop of interstage voltage

achieved time resolution 330 ps